Optical Coherence Tomography Angiography Quantitative Assessment of Macular Neovascularization in Best Vitelliform Macular Dystrophy

Maurizio Battaglia Parodi, Alessandro Arrigo, and Francesco Bandello

Department of Ophthalmology, IRCCS, Ospedale San Raffaele, Vita-Salute San Raffaele University, Milan, Italy

Correspondence: Alessandro Arrigo, Department of Ophthalmology, University Vita-Salute, Ospedale San Raffaele, Via Olgettina 60, 20132, Milan, Italy; alessandro.arrigo@hotmail.com.

Received: February 26, 2020
Accepted: June 3, 2020
Published: June 30, 2020

Citation: Battaglia Parodi M, Arrigo A, Bandello F. Optical coherence tomography angiography quantitative assessment of macular neovascularization in best vitelliform macular dystrophy. *Invest Ophthalmol Vis Sci.* 2020;61(6):61. https://doi.org/10.1167/iovs.61.6.61

Purpose. To describe quantitative characteristics of macular neovascularization (MNV) in vitelliform macular dystrophy (VMD) patients by means of optical coherence tomography angiography (OCTA).

Methods. The study design was a prospective case series. All patients underwent complete ophthalmologic assessment, optical coherence tomography, and OCTA. The quantitative OCTA parameters examined included vessel tortuosity and vessel dispersion of the MNV. The primary outcome was OCTA characterization of MNV in VMD. Secondary outcomes included the evolution of MNV over the follow-up.

Results. A total of 78 eyes were recruited for the study. MNV was identified in 50 eyes (64%) at baseline and in 51 eyes (65%) at the end of the follow-up (mean follow-up, 24.7 ± 9.7 months). MNV was detected in four out of the 30 eyes classified as stages 2 and 3 (13%), showing exudative manifestations and undergoing ranibizumab treatment, leading to clinical stabilization. OCTA detected MNV in 46 out of 48 eyes (96%) classified as stages 4 and 5, showing no evidence of exudative manifestation. All of the non-exudative MNVs were merely observed over the follow-up and received no treatment. At the end of the follow-up, 47 out of 48 eyes displayed MNV (98%). Non-exudative MNVs remained stable over the follow-up. Statistically significant differences were found when comparing vessel tortuosity and vessel dispersion in the two MNV subforms.

Conclusions. VMD is characterized by two MNV subforms. Exudative MNV is rare and may develop in the early stages of the disease, in association with bleeding and fluid formation. Non-exudative MNV develops very commonly in the advanced stage of VMD, without any exudative manifestation.

Keywords: Best vitelliform macular dystrophy, macular neovascularization, optical coherence tomography angiography

Best vitelliform macular dystrophy (VMD) can show mutable phenotypic manifestations over its natural evolution from the initial vitelliform stage toward a gradual reabsorption of vitelliform material and up to atrophic changes.[1–10] Macular neovascularization (MNV) can complicate the course of VMD and may contribute toward a further deterioration in visual acuity.[1,2,11,12] The diagnosis of MNV complicating VMD is often not straightforward.[11] It is generally based on the biomicroscopic identification of subretinal fluid and/or retinal or subretinal hemorrhages and on the detection of dye leakage on fluorescein angiography (FA). The recent introduction of optical coherence tomography angiography (OCTA) has refined our understanding of the vascular network alterations at the level of the retina and the choriocapillaris in VMD and indicates that MNV is more frequent than previously thought, especially in the advanced stages of the disease.[12,13] To our knowledge, no study has explicitly analyzed the quantitative characteristics of MNV related to VMD in an attempt to define specific subforms. The purpose of the present study was to delineate the quantitative OCTA parameters of MNV secondary to VMD.

Methods

The design of the study was a prospective case series that enrolled consecutive patients affected by VMD examined at the Ophthalmology Department of San Raffaele Hospital in Milan between January 2015 and June 2017. The protocol was approved by the institutional review board, and the procedures followed the tenets of the Declaration of Helsinki. Written informed consent was obtained from all subjects. Inclusion criteria were a clinical diagnosis of VMD confirmed by identification of mutations in the *BEST1* gene, along with clear media and stable fixation that would allow precise OCTA examination. The exclusion criterion was the identification of any other ocular disorder. VMD classification included eyes in stage 1 (previtelliform/subclinical, with no biomicroscopic alterations), stage 2 (vitelliform),

stage 3 (pseudohypopyon), stage 4 (vitelliruptive/scrambled egg), and stage 5 (atrophic/cicatricial),[1,2] but only patients in stages 2 to 5 were involved in the study.

Each patient underwent a complete ophthalmic examination, including best-corrected visual acuity (BCVA) on standard Early Treatment Diabetic Retinopathy Study charts, color photography, fluorescein angiography, spectral-domain optical coherence tomography (SD-OCT) (Spectralis HRA; Heidelberg Engineering, Heidelberg, Germany), and OCTA (Swept Source DRI OCT Triton; Topcon Corporation, Tokyo, Japan). In addition, a subset of patients also underwent indocyanine green angiography (ICGA), as an ancillary examination. The patients received a follow-up examination every 6 months, with the opportunity to have additional visits if necessary.

MNV was identified on OCTA by detecting a neovascular net in the outer retinal en face slab (outer plexiform layer to Bruch's membrane) and in the choriocapillaris slab, as assessed by two experienced retina specialists (A.A., F.B.) employing the 3 × 3-mm scan, which ensured the highest resolution. MNV was considered exudative when dye leakage was detected on FA and when subretinal fluid extending beyond the area of the VMD lesion was found on OCT, along with the possible presence of retinal/subretinal hemorrhages.

Automatic segmentations of the superficial capillary plexus (SCP), deep capillary plexus (DCP) and choriocapillaris (CC) were obtained from OCTA acquisitions (4.5 × 4.5-mm scan centered on the fovea) to calculate vessel density (VD). Each segmentation was carefully inspected and, if necessary, manually corrected by two expert ophthalmologists (M.B.P., A.A.), taking into consideration only high-quality images (Topcon quality index > 80). All OCTA images were captured by two ophthalmologists (M.B.P., A.A.) at least twice in order to assess both reproducibility and repeatability. All reconstructions were loaded in ImageJ software (National Institutes of Health, Bethesda, MD, USA)[14] to calculate VD. The "Adjust threshold" tool was used in ImageJ to highlight the blood vessels and to reduce the noise. The method pipeline employed ran as follows: import .tiff image → adjust → threshold → automatic threshold → mean thresholding → export binarized image. After the "mean threshold" image binarization, VD was calculated to determine the proportion of white pixels compared to black. The foveal avascular zone was manually segmented and excluded.

Distinct quantitative OCTA parameters were adopted in order to analyze the MNV characteristics, including vessel tortuosity (VT) and vessel dispersion (VDisp), which are already employed in assessing other pathological conditions.[15–18] In short, VT is defined as the ratio of the shortest pathway to the straight-line length[19] and provides information about vascular perfusion.[20,21] VDisp is defined as a measure of the space-filling of a given vascular tree[22] and provides information about the vascular network disorganization.[23] MNV was extracted from the 3 × 3-mm OCTA reconstruction, corrected to assess the vertical extension of the lesion.[16]

The control group consisted of 40 healthy volunteers matched for age, sex, axial length, and refractive error. All of the control subjects underwent an ophthalmologic examination, complete with SD-OCT and OCTA. Axial length was measured by means of the IOLMaster 500 (Carl Zeiss Meditec, Jena, Germany) in both patients and control subjects, and refractive error was calculated using a Nidek AR-1 Auto Refractometer (Nidek, Aichi, Japan).

The primary outcome measure was the assessment of quantitative parameters of MNV secondary to VMD in different stages of the disease performed by means of OCTA. Secondary outcomes included the evolution of the MNV over the follow-up. The statistical analyses were performed using unpaired Student's *t*-tests (SPSS Statistics; IBM, Armonk, NY, USA), with statistical significance set at $P < 0.05$. Differences between the two groups in BCVA, VD, VT, VDisp, and MNV size were investigated with a linear mixed model. In the model, the aforementioned variables were the dependent variable, the group was the covariate, and the random effects had a nested design and included the family ID and patient ID to account for within-family and within-subject correlations. This specific analysis was performed with R 3.3.2 (R Foundation for Statistical Computing, Vienna, Austria). Intergrader agreement was assessed with intraclass correlations, whereas repeatability and reproducibility were calculated for each OCTA parameter.

Results

Seventy-eight eyes of 39 patients from 26 families affected by genetically confirmed VMD were recruited for the study. The demographic and clinical characteristics of patients and control subjects are listed in Table 1. In this case series, both eyes of each patient belonged to the same stage, with complete phenotypic inter-eye correlation. Overall, mean follow-up was 24.7 ± 9.7 months (range, 18–48 months). The control group consisted of 40 healthy subjects, with a mean age of 36 ± 15 years (Table 1). Mean axial lengths were 23.10 ± 0.82 mm and 23.00 ± 0.77 mm in patients and control subjects, respectively.

OCTA identified MNV with subfoveal location in 50 out of 78 eyes (64%) at baseline and in 51 eyes (65%) at the end of the follow-up. Table 2 correlates the presence of MNV according to the specific VMD stage at the moment of the diagnosis. In order to simplify the statistical analyses and interpretation of the results, we combined stages 2 and 3 and stages 4 and 5.

MNV was found in four out of 30 eyes (13%) in stages 2 and 3 (three eyes in stage 2 and one eye in stage 3); in all four eyes, MNV included exudative manifestations, exhibiting dye leakage on FA, subretinal fluid extending beyond the area of the vitelliform lesion on structural OCT, and subretinal hemorrhage (Fig. 1). MNV was found in both eyes of a single patient and in a single eye of another two patients and was diagnosed in two eyes after 5 months of follow-up and in another two cases after 7 and 9 months, respectively. OCTA quantitative assessment of the MNV revealed a baseline mean VT value of 9.2 and a baseline mean VDisp of 51 (Table 3). All four eyes presenting with exudative MNV underwent intravitreal ranibizumab injection and achieved a stable lesion with a single treatment. No further reactivation (no exudative signs) was registered over a mean follow-up of 39 ± 3.4 months (range, 36–42 months). At the end of the follow-up period, no statistically significant change was registered in either VT or VDisp (Table 3). Mean visual acuity of the four eyes with exudative MNV was 0.1 ± 0.1 logMAR (approximately corresponding to 20/25 Snellen equivalent) before the development of MNV. This value dropped down to 0.75 ± 0.1 logMAR (20/110 Snellen equivalent) at the onset of the MNV, improved to 0.2 ± 0.05 logMAR (20/32 Snellen equivalent) after anti-vascular endothelial growth factor (VEGF) injection, and remained stable over the follow-up.

Investigative Ophthalmology & Visual Science

Table 1. Demographic and Clinical Characteristics of Patients Affected by VMD and of the Control Subjects

		BVMD Stage				
	Patients	2	3	4	5	Controls
Patients (*n*)	39	14	2	20	4	40
Eyes (*n*)	78	26	4	40	8	80
Age (y), mean ± SD	37 ± 18	36 ± 19	36 ± 32	38 ± 16	38 ± 23	36 ± 15
Males, *n* (%)	23 (59)	8 (57)	2 (100)	10 (50)	3 (75)	45 (56)
LogMAR BCVA, mean ± SD (Snellen equivalent)	0.36 ± 0.31 (20/45)	0.24 ± 0.22 (20(37)	0.26 ± 0.27 (20/36)	0.36 ± 0.29 (20/45)	0.82 ± 0.32 (20/125)	0.0 ± 0.0 (20/20)

Table 2. Choroidal Neovascularization and Atrophy at the End of Follow-Up in the Different Stages of VMD

	Stage 2 (26 Eyes)	Stage 3 (4 Eyes)	Stage 4 (40 Eyes)	Stage 5 (8 Eyes)
Macular neovascularization, *n*	3	1	40	7
Atrophy, *n*	0	0	0	1

With regard to the remaining 48 eyes of the 24 patients classified as stages 4 and 5, OCTA detected a neovascular net in the outer retinal en face slab and the choriocapillaris slab, consistent with the diagnosis of MNV, in 46 eyes (96%). No evidence of exudative manifestation was visible on biomicroscopy, and no leakage was detectable on FA. ICGA, performed as an ancillary examination in 10 patients, revealed fine vascular alterations in the early phases, with staining in the late phases (Fig. 2) that could not be promptly identified as MNV. Structural SD-OCT revealed fluid within the limit of the vitelliform lesion in 36 eyes (78%) but failed to find any subretinal fluid external to the lesion (Fig. 2). Another eye developed MNV with non-exudative manifestations over the follow-up (Fig. 3). This meant that by the end of the follow-up 47 out of 48 eyes displayed MNV (98%). Throughout the follow-up, no evidence of exudation was identified in any of the 47 eyes, which remained clinically stable. Quantitative OCTA assessment of the MNV revealed a mean VT value of 6.8 and a mean VDisp value of 22.9 (Table 3). No statistically significant change was detected at the end of the follow-up in either VT or VDisp.

Mean visual acuity values for the eyes with non-exudative MNV were 0.45 ± 0.34 logMAR and 0.45 ± 0.33 logMAR (approximately corresponding to 20/55 Snellen equivalent) at baseline and final examinations, respectively. The MNV in stages 2 and 3 revealed higher values of VT, VDisp, and size than MNV in stages 4 and 5, the difference being statistically significant (Table 3). VD calculated in the 3 × 3-mm area of the SCP, DCP, and CC turned out to be lower in patients than in the control subjects (Table 4). Intraclass correlation assessments found an intergrader agreement of 95%. Repeatability and reproducibility were calculated for each OCTA parameter. Overall, repeatability ranged from 88% to 97%, and reproducibility ranged from 88% to 98% (Tables 3 and 4).

Discussion

VMD is a very complex inherited disorder, related in most cases to mutations of the *BEST1* gene.[2,24] Typically, VMD is characterized by high phenotypic heterogeneity and variable clinical manifestations.[1–11] MNV has been previously described as a possible complication, especially in the early stages of VMD.[1,2,10–13,25,26] In most cases, exudative manifestations due to MNV activity have been treated with anti-VEGF intravitreal injections, with positive outcomes.[11,25,26] The present study, based on OCTA assessment, revealed that MNV is actually a quite frequent manifestation of VMD, occurring in about two-thirds of cases overall. In fact, two different MNV subtypes can be identified: an exudative MNV, which is typical of early stages (stages 2 and 3), and a non-exudative MNV, which can be detected in almost all eyes in the more advanced stages. Our previous cross-sectional study revealed MNV in 87% of eyes in stages 4 and 5,[13] but the more precise technical equipment employed in association with the longitudinal follow-up enabled MNV to be identified in 96% of eyes in stages 4 and 5 in the present investigation. MNV has traditionally been identified in VMD by detecting biomicroscopic evidence of subretinal fluid and/or macular hemorrhages, in association with dye leakage on FA. However, it is practically impossible to detect non-exudative MNV on either FA or ICGA, due to staining of the vitelliform deposits.[11,27] OCTA can provide a more

Table 3. OCT Angiography Quantitative Parameters in Eyes Affected by VMD Complicated by MNV and in Eyes of Control Subjects

	MNV Stages			*P*				
	2 and 3 (1)	4 and 5 (2)	Controls (3)	1 vs. 2	1 vs. 3	2 vs. 3	Reproducibility (%)	Repeatability (%)
VT								
Baseline	9.2 ± 0.6	6.8 ± 0.4	N/A	<0.0001	N/A	N/A	95	96
Final	8.5 ± 0.5	6.8 ± 0.5	N/A	<0.0001	N/A	N/A	95	95
VDisp								
Baseline	51.1 ± 8.9	23.9 ± 4.4	N/A	<0.0001	N/A	N/A	89	88
Final	49.2 ± 7.5	23.9 ± 4.4	N/A	<0.0001	N/A	N/A	90	88
Area (μm^2)								
Baseline	1088.8 ± 187.2	651.6 ± 188.4	N/A	<0.0001	N/A	N/A	92	94
Final	1159 ± 245.2	731.7 ± 242.2	N/A	0.0023	N/A	N/A	92	94

Investigative Ophthalmology & Visual Science

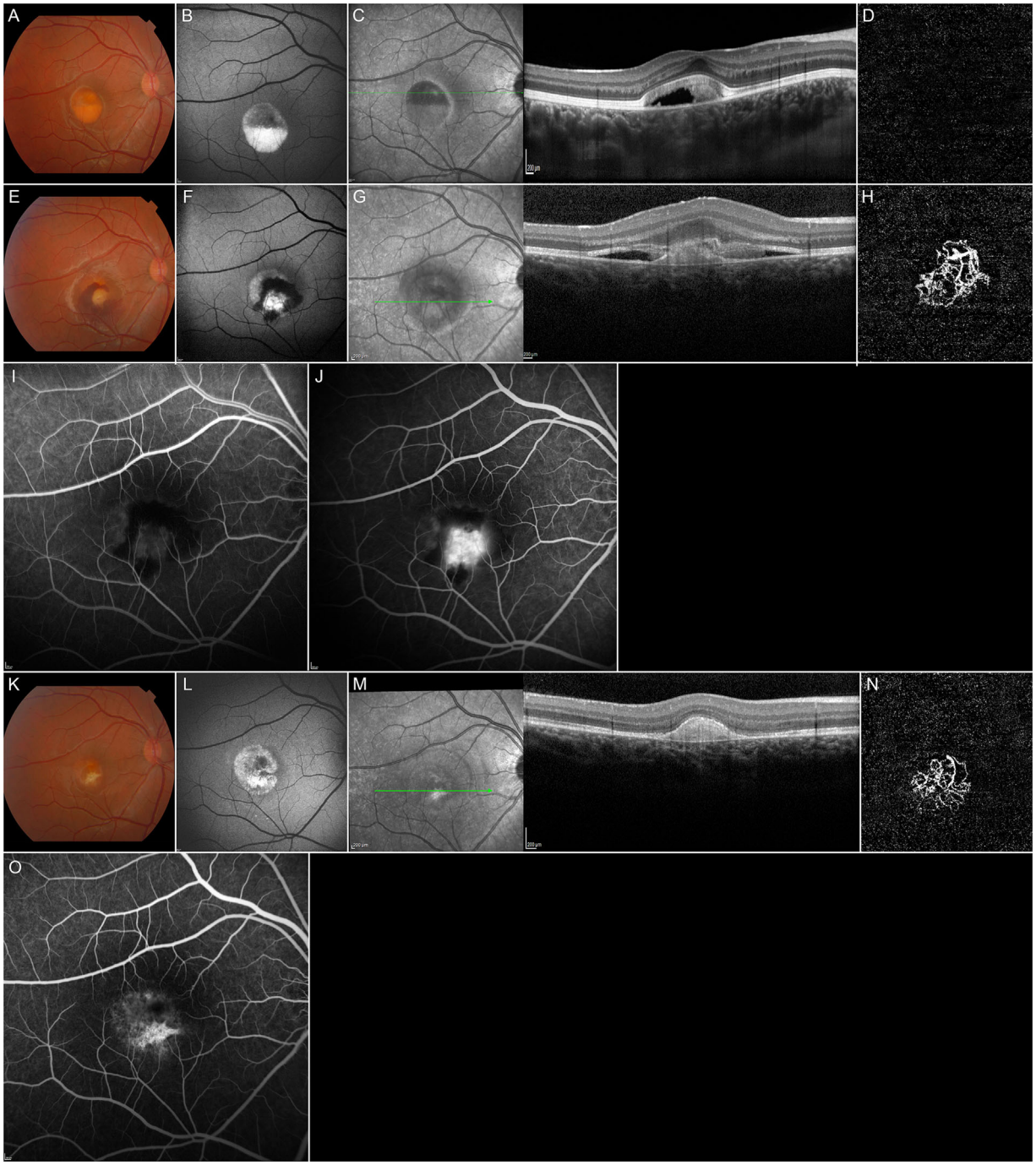

Figure 1. Exudative MNV in Best VMD. Color fundus (**A**) and fundus autofluorescence (**B**) images showed subretinal hemorrhage in stage 2 Best VMD. Structural OCT (**C**) revealed subretinal exudation, and OCTA (**D**) delineated the macular neovascularization pattern. After anti-vascular endothelial growth factor treatment, both color fundus (**E**) and fundus autofluorescence (**F**) showed reabsorption of fluid and blood. Structural OCT (**G**) revealed no sign of exudation, and OCTA (**H**) revealed a reduction in the size of the macular neovascularization.

reliable assessment, owing to the absence of dye leakage and staining.

OCTA quantitative assessment revealed that exudative MNV in stages 2 and 3 is characterized by higher values of both VT and VDisp than non-exudative MNV in stages 4 and 5, suggesting a more florid neovascular network with high perfusion and high vascular disorganization in former MNV. Interestingly, exudative MNV related to VMD displays VT and VDisp values similar to those typical of type 2 MNV secondary to AMD.[14]

At present, little is known of the pathogenesis of MNV secondary to VMD, which has been related to retinal pigment epithelium (RPE) alterations associated with local hypoperfusion.[11–13] The identification of two MNV subforms with different quantitative parameters may provide some clues on the possible pathogenesis. The exudative MNV is characterized by higher VT, higher VDisp, and larger size, whereas the VD of the three vascular plexa in the 3 × 3-mm area was similar to that found in the non-exudative MNV. This might suggest that exudative MNV is associated with a

Investigative Ophthalmology & Visual Science

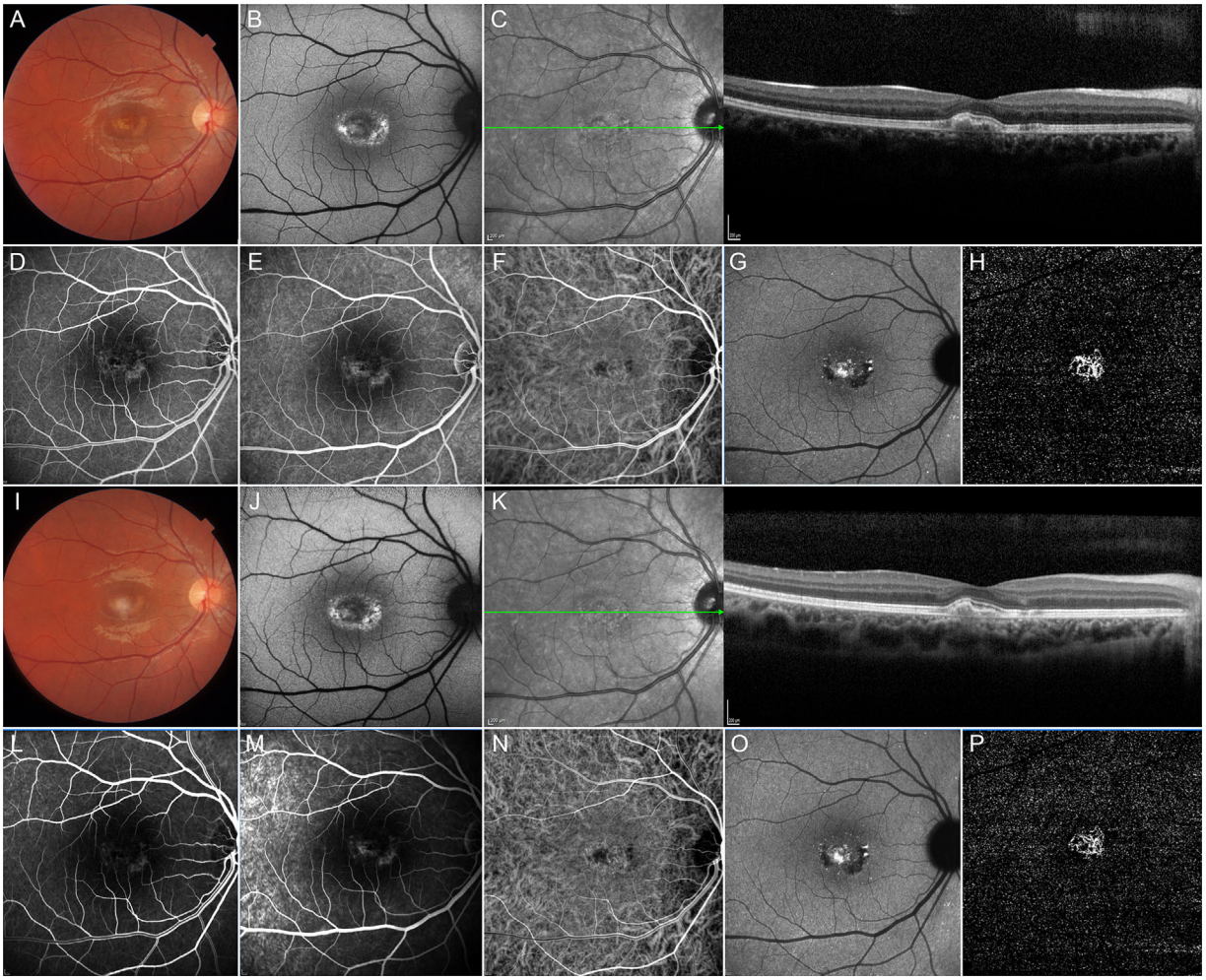

Figure 2. Non-exudative MNV in Best VMD. Color fundus (**A**), fundus autofluorescence (**B**), and OCT (**C**) showed stage 4 Best vitelliform macular dystrophy. OCTA (**D**) revealed MNV. Over the follow-up, color fundus (**E**), fundus autofluorescence (**F**), OCT (**G**), and OCTA (**H**) images indicated no changes.

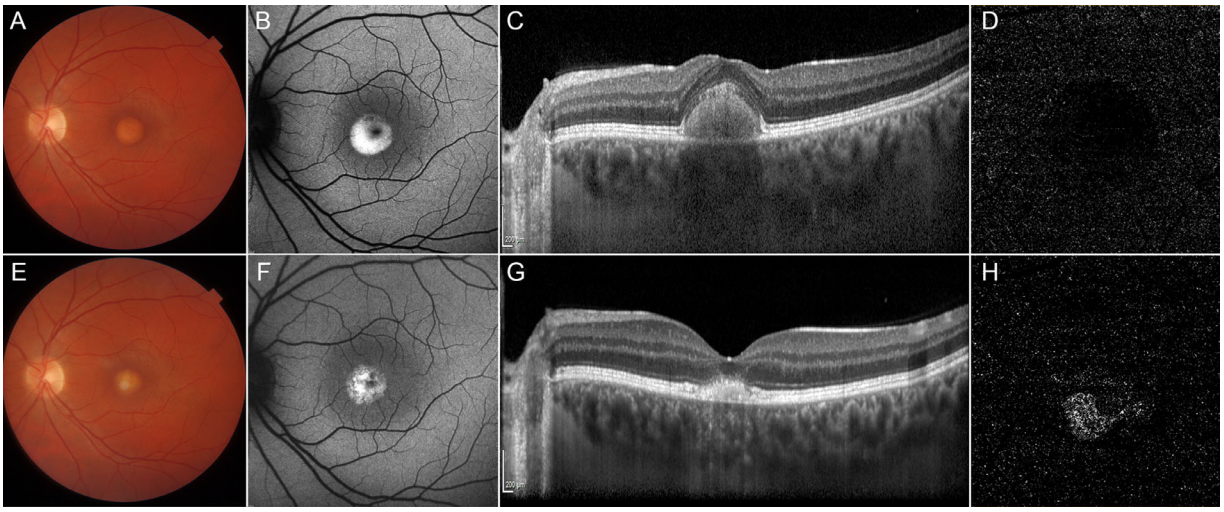

Figure 3. Development of MNV in Best VMD over the follow-up. Color fundus (**A**), fundus autofluorescence (**B**), and OCT (**C**) showed stage 2 Best VMD. OCTA (**D**) showed the absence of MNV. After 1 year, both color fundus (**E**) and fundus autofluorescence (**F**) revealed that the condition had evolved toward stage 4 Best VMD, whereas structural OCT (**G**) showed exudation and OCTA (**H**) identified MNV.

Investigative Ophthalmology & Visual Science

Table 4. OCTA Vessel Density Analyses in Eyes Affected by VMD Complicated by MNV and in Eyes of Control Subjects

	MNV Stage (%), Mean ± SD			P				
Vessel Density	Stages 2 and 3 (1)	Stages 4 and 5 (2)	Controls (3)	1 vs. 2	1 vs. 3	2 vs. 3	Reproducibility (%)	Repeatability (%)
SCP								
Baseline	0.36 ± 0.03	0.39 ± 0.03	0.42 ± 0.01	0.047	<0.0001	<0.0001	94	95
Final	0.38 ± 0.04	0.40 ± 0.04		0.52	<0.0001	<0.0001	94	96
DCP								
Baseline	0.37 ± 0.01	0.38 ± 0.03	0.41 ± 0.01	0.39	<0.0001	<0.0001	94	95
Final	0.38 ± 0.02	0.38 ± 0.03		0.80	<0.0001	<0.0001	93	95
CC								
Baseline	0.47 ± 0.04	0.47 ± 0.02	0.5 ± 0.01	0.62	<0.0001	<0.0001	98	97
Final	0.46 ± 0.02	0.46 ± 0.03		0.58	<0.0001	<0.0001	98	97

rapidly growing neovascular network, possibly related to a cytokine/trophic factor imbalance triggered by the progressive accumulation of vitelliform material and occurring in a limited number of eyes in the early stage of the disease. On the other hand, non-exudative MNV, characterized by lower perfusion and lower vascular disorganization, as shown by the reduced VT and VDips values, may develop more slowly, stimulated by the trophic demand of the outer retina that is due to the increasingly impaired metabolic exchanges between the RPE and photoreceptor outer segments.

Remarkably, non-exudative MNV can be visualized on OCTA in the more advanced stages, when the vitelliform material is progressively removed. Nevertheless, our data do not enable us to be more precise regarding the emergence of non-exudative MNV. It is plausible that the neovascular growth during the advanced stages could be part of a gradual process that may even have its origins in an earlier stage, but the technical limitations of the diagnostic tools that are currently available, including FF, ICGA, and OCTA, prevent us from visualizing an emerging MNV when the vitelliform material is still dense and abundant. Similarly, it stands to reason that MNV should tend to evolve toward atrophic changes in stage 5, becoming no longer detectable over a long-term follow-up.

Identifying the specific characteristics of MNV may prove useful in the practical management of VMD. Exudative MNV shows higher values of VT and VDisp than the non-exudative subform, both before and after treatment, making identification easier even in the advanced stages. Whereas previous reports have endorsed anti-VEGF treatment for exudative MNV,[11,25,26] the stability displayed by non-exudative MNV (no exudative manifestations and no substantial changes in quantitative OCTA vascular parameters) suggests that anti-VEGF is unnecessary and may even be harmful in non-exudative MNV, potentially accelerating atrophic changes with consequent functional deterioration. Moreover, in view of the prospective new therapies,[28] it is essential to be in possession of a full and accurate picture of the clinical characteristics over the course of VDM so as to be able to identify the most appropriate approach and time frame.

We acknowledge that this investigation has several limitations, especially in view of the small number of patients included in the study and the relatively short and uneven follow-up. In addition, we included both of the eyes of the same patient in the statistical analyses, creating the basis for an inherent bias,[29] even though the statistical power was improved by using a linear mixed model to manage the data. Moreover, the technical shortcomings of the OCTA resolution may have prevented a very early and indistinct MNV being detected. It is therefore difficult to pinpoint just when the MNV detected on OCTA in stages 4 and 5 (when the vitelliform material gradually fades away) actually begins. It is theoretically possible for a thin MNV to originate in stages 2 and 3, becoming OCTA detectable later. The quantitative OCTA parameters adopted in this study were derived from our experience with other conditions and can be further improved in the future as technology evolves. We should also point out that our investigation was based on VMD cases related to *BEST1* mutations and might not prove to be applicable to all VMD genotypes. VMD is quite a rare disease, which makes collecting a sufficiently large sample and establishing a long follow-up a considerable challenge. This study should therefore be regarded as merely a primary analysis designed to prompt further research into the identification and evolution of MNV in VMD.

In conclusion, our study demonstrates that VMD can be associated with two different MNV subtypes on OCTA. The initial stages of VMD can be complicated by the onset of exudative MNV, characterized by high VT and Vdisp on OCTA, whereas more advanced stages are characterized by non-exudative MNV, showing lower VT and VDisp. Identifying MNV related to VMD can have direct implications for the final anatomical and functional prognosis, as well as for the appropriate therapeutic response, especially in view of forthcoming treatments.

Acknowledgments

The authors thank Alessandro Rabiolo, MD, for providing assistance in the statistical analyses.

Disclosure: **M. Battaglia Parodi**, None; **A. Arrigo**, None; **F. Bandello**, Alcon (C), Alimera Sciences (C), Allergan, Inc. (C), Farmila Théa (C), Bausch & Lomb (C), Genentech (C), Hoffmann-La Roche (C), Novagali Pharma (C), Novartis (C), Bayer Shering Pharma (C), Sanofi-Aventis (C), Thrombogenics (C), Carl Zeiss, Inc. (C), Pfizer (C), Santen Pharmaceutical (C), SIFI (C)

References

1. Gass JDM. Best's disease. In: Gass J , ed. *Stereoscopic Atlas of Macular Diseases. Diagnosis and Treatment*, Vol. 1, 4th ed. St. Louis, MO: Mosby; 1997:304–311.

2. Boon CJ, Klevering BJ, Leroy BP, et al. The spectrum of ocular phenotypes caused by mutations in the BEST1 gene. *Prog Retin Eye Res*. 2009;28:187–205.
3. Kay DB, Land ME, Cooper RF, et al. Outer retinal structure in Best vitelliform macular dystrophy. *JAMA Ophthalmol*. 2013;131:1207–1215.
4. Duncker T, Greenberg JP, Ramachandran R, et al. Quantitative fundus autofluorescence and optical coherence tomography in Best vitelliform macular dystrophy. *Invest Ophthalmol Vis Sci*. 2014;55:1471–1482.
5. Battaglia Parodi M, Iacono P, Campa C, et al. Fundus autofluorescence patterns in Best vitelliform macular dystrophy. *Am J Ophthalmol*. 2014;158:1086–1092.
6. Battaglia Parodi M, Sacconi R, Iacono P, et al. Choroidal thickness in Best vitelliform macular dystrophy. *Retina*. 2016;36:764–769.
7. Battaglia Parodi M, Iacono P, Romano F, Bandello F. Spectral domain optical coherence tomography features in different stages of Best vitelliform macular dystrophy. *Retina*. 2018;38:1041–1046.
8. Battaglia Parodi M, Castellino N, Iacono P, et al. Microperimetry in Best vitelliform macular dystrophy. *Retina*. 2018;38:841–848.
9. Battaglia Parodi M, Romano F, Arrigo A, et al. Natural course of the vitelliform stage in Best vitelliform macular dystrophy: a five-year follow-up study. *Graefes Arch Clin Exp Ophthalmol*. 2020;258:297–301.
10. Augstburger E, Orès, Mohand-Said S, et al. Outer retinal alterations associated with visual outcomes in Best vitelliform macular dystrophy. *Am J Ophthalmol*. 2019;208:429–437.
11. Khan KN, Mahroo OA, Islam F, et al. Functional and anatomical outcomes of choroidal neovascularization complicating BEST1-related retinopathy. *Retina*. 2017;37:1360–1370.
12. Guduru A, Gupta A, Tyagi M, et al. Optical coherence tomography angiography characterization of Best disease and associated choroidal neovascularisation. *Br J Ophthalmol*. 2018;102:444–447.
13. Battaglia Parodi M, Romano F, Cicinelli MV, et al. Retinal vascular impairment in Best vitelliform macular dystrophy assessed by means of optical coherence tomography angiography. *Am J Ophthalmol*. 2018;187:61–70.
14. Schindelin J, Arganda-Carreras I, Frise E, et al. Fiji: an open-source platform for biological-image analysis. *Nat Methods*. 2012:9:676–682.
15. Arrigo A, Aragona E, Capone L, et al. Advanced optical coherence tomography angiography analysis of age-related macular degeneration complicated by onset of unilateral choroidal neovascularization. *Am J Ophthalmol*. 2018;195:233–242.
16. Arrigo A, Romano F, Aragona E, et al. Optical coherence tomography angiography can categorize different subgroups of choroidal neovascularization secondary to age-related macular degeneration. *Retina*. 2020; doi:10.1097/IAE.0000000000002775.
17. Arrigo A, Romano F, Aragona E, et al. OCTA-based identification of different vascular patterns in Stargardt disease. *Transl Vis Sci Technol*. 2019;8:26.
18. Arrigo A, Romano F, Albertini G, et al. Vascular patterns in retinitis pigmentosa on swept-source optical coherence tomography angiography. *J Clin Med*. 2019;8:1425.
19. Adler PM. *Porous Media: Geometry and Transports*. Stoneham, MA: Butterworth-Heinemann;1992.
20. Tomita Y, Kubis N, Calando Y. Long-term in vivo investigation of mouse cerebral microcirculation by fluorescence confocal microscopy in the area of focal ischemia. *J Cereb Blood Flow Metab*. 2005;25:858–967.
21. Goldman D, Popel AS. A computational study of the effect of capillary network anastomosis and tortuosity on oxygen transport. *J Theor Biol*. 2000;206:181–194.
22. Righi M, Locatelli SM, Carlo-Stella C, et al. Vascular amounts and dispersion of caliber-classified vessels as key parameters to quantitate 3D micro-angioarchitectures in multiple myeloma experimental tumors. *Sci Rep*. 2018;8:17520.
23. Konerding MA, Malkusch W, Klapthor B, et al. Evidence for characteristic vascular patterns in solid tumours: quantitative studies using corrosion casts. *Br J Cancer*. 1999;80:724–732.
24. Stone EM, Nichols BE, Streb LM, et al. Genetic linkage of vitelliform macular degeneration (Best's disease) to chromosome 11q13. *Nat Genet*. 1992;1:246–250.
25. Shahzad R, Siddiqui MA. Choroidal neovascularization secondary to Best vitelliform macular dystrophy detected by optical coherence tomography angiography. *JAAPOS*. 2017;21:68–70.
26. Patel RC, Gao SS, Zhang M, et al. Optical coherence tomography angiography of choroidal neovascularization in four inherited retinal dystrophies. *Retina*. 2016;36:2339–2347.
27. Battaglia Parodi M, Iustulin D, Russo D, et al. Adult-onset foveomacular vitelliform dystrophy and indocyanine green videoangiography. *Graefes Arch Clin Exp Ophthalmol*. 1996;234:208–211.
28. Guziewicz KE, Cideciyan AV, Beltran WA, et al. *BEST1* gene therapy corrects a diffuse retina-wide microdetachment modulated by light exposure. *Proc Natl Acad Sci USA*. 2018;115:E2839–E2848.
29. Murdoch IE, Morris SS, Cousens SN. People and eyes: statistical approaches in ophthalmology. *Br J Ophthalmol*. 1998;82:971–973.

Investigative Ophthalmology & Visual Science